

OPTIMAL THICKNESS AND DEPTH FOR EMBEDDED PIEZOELECTRIC ACTUATORS

Kegong Wu¹, Hartmut Janocha²

*Laboratory for Process Automation (LPA)
Saarland University, Building 13
D-66123 Saarbrücken, Germany*

This paper uses classical beam theory to analyze the actuating capabilities of the embedded piezoelectric elements in beam structures. After considering the piezoelectric effect of piezoelectric material, the moment equation for finding the optimal thickness and depth of embedded piezoelectric actuators is set up. The optimal configurations of the embedded piezoelectric actuators can be then obtained by solving the equation. Two and three-dimensional contour maps and plots are also presented for different modulus ratios between the base material and piezoelectric material, which are used to show the best configurations for so-called smart beams with embedded piezoelectric actuators. The results are afterwards extended to the case of smart plates. It is shown that both of the thickness and the depth of embedded piezoelectric material as well as the modulus ratio (in the plate case, also the Poisson ratio) between the base material and piezoelectric material have great influence on the actuating capabilities of the embedded piezoelectric elements.

Keywords: *piezoelectric actuator, embedded ceramics, optimal thickness, optimal depth*

1 Introduction

Piezoelectric material, such as sintered lead-zirconium-titanate (PZT) ceramics and polyvinyl fluoride (PVDF) films, can be produced to work as both actuators and sensors, due to their properties of inverse piezoelectric effect and direct piezoelectric effect [1]. They have been used successfully for many years in the field of vibration control [2], but the early studies [3] are mostly focused on surface glued piezoelectric material, which exhibit some disadvantages, such as the difficulties to protect the ceramics and the connection wires, bad coupling with only one surface glued on the base material, etc. These disadvantages can be overcome by embedding the piezoelectric material inside the structures. Furthermore, the optimal positions, especially with respect to the depth [4] of the piezoelectric material, can be calculated for enhancing the actuation effect and sensor signal. As this paper shows, the thickness of the piezoelectric actuators plays also an important role when they are embedded.

The moment equation of the piezoelectric actuator is firstly derived using classical beam theory following the strain and stress distribution analysis. Then, the optimal thickness and depth of the embedded piezoelectric actuator are obtained from this moment equation. In order to assure the piezoelectric material embedded inside the base structure, the conditions to

achieve the optimal thickness and depth are also written out respectively. Two and three-dimensional contour maps and plots are also presented with different modulus ratios between the base material and piezoelectric material, which are used to show the best configurations for so-called smart beams with embedded piezoelectric actuators. And at last, the conclusions are also extended to the case of smart plates, in which the piezoelectric actuators are embedded.

2 Strain and stress distribution in the smart beam

Figure 1 shows the strain distribution induced by the moment in the smart beam structure, when the piezoelectric actuator intends to elongate with the external voltage. In Fig. 1, t and T are the half thicknesses of the piezoelectric material and of base structure, respectively, d is the distance between the neutral plane of the beam structure and the center plane of the piezoelectric material, and M shows the moment induced by the piezoelectric actuator. The axial force, which has always the same value for the same thickness, is omitted, because only the moment effect is discussed. The strain is continuous and has linear relationship in the whole structure (see Fig. 1), with the assumption that the influence of the piezoelectric material to the neutral plane of the beam structure is neglectable.

¹ PhD. Student, k.wu@lpa.uni-saarland.de

² Professor, janocha@lpa.uni-saarland.de

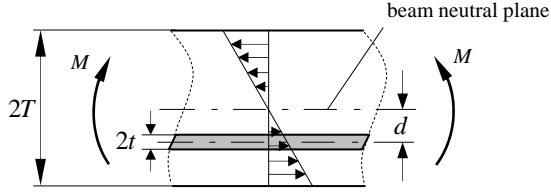


Figure 1: Strain distribution in the smart beam

The stress distribution in the base material remains consistent with the strain distribution, but the stress distribution in the piezoelectric material is however not the same as strain distribution due to the difference of the elastic moduli of the different material and the actuation function of the piezoelectric material. In the case mentioned above, the stress distribution is shown as Fig. 2.

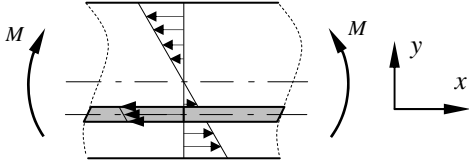


Figure 2: Stress distribution in the smart beam

3 Moment generated by the piezoelectric actuator

After the strain and stress distribution analyze, the strain of the base structure ε_s and the strain of the piezoelectric actuator ε_p can be written as

$$\varepsilon_s = \varepsilon_p = \frac{y}{\rho}. \quad (1)$$

Here, y is the distance from the place, where the strain occurs, to the neutral plane of the beam structure, and ρ is the curvature radius of the beam structure when it bends. The stress of the base material σ_s can then be shown as Eq.(2). E_s is the elastic modulus of the base material.

$$\sigma_s = E_s \varepsilon_s = \frac{E_s y}{\rho} \quad (2)$$

And the stress in the piezoelectric material σ_p , shown as Eq. (3), can be deduced from the piezoelectric effect, shown as Eq.(4) [5]. Where E_p is the elastic modulus of the piezoelectric material, d_{31} and \mathbf{E} are the charge constant of the piezoelectric material and the driving electric field of the piezoelectric actuator, respectively.

$$\sigma_p = \frac{E_p y}{\rho} - E_p d_{31} \mathbf{E} \quad (3)$$

$$\varepsilon_p = \frac{\sigma_p}{E_p} + d_{31} \mathbf{E} \quad (4)$$

The moment M that the piezoelectric actuator generated to drive the smart beam can then be derived with integration, shown as Eq.(5), for the stress from piezoelectric actuator, which has the inverse direction to Eq.(3). Where b is the width of the piezoelectric material.

$$\begin{aligned} M &= b \int_{-d-t}^{-d+t} -\sigma_p y \, dy \\ &= b \int_{-d-t}^{-d+t} E_p \left(d_{31} \mathbf{E} - \frac{y}{\rho} \right) y \, dy \quad (5) \\ &= -b E_p t \left(2d d_{31} \mathbf{E} + \frac{6d + 2t}{3\rho} \right) \end{aligned}$$

And then, with the consideration that the curvature radius of the beam can be written as Eq.(6), and together with the inertia moment of the beam I_y , shown as Eq.(7), the moment M can be at last obtained as Eq.(8). Where B is the width of the beam.

$$\rho = \frac{E_s I_y}{M} \quad (6)$$

$$I_y = \frac{B(2T)^3}{12} \quad (7)$$

$$M = \frac{-2E_p E_s B T^3 \mathbf{E} b d_{31} t}{E_s B T^3 + 3E_p b t d^2 + E_p b t^3} \quad (8)$$

4 Optimal thickness and depth of the piezoelectric actuators

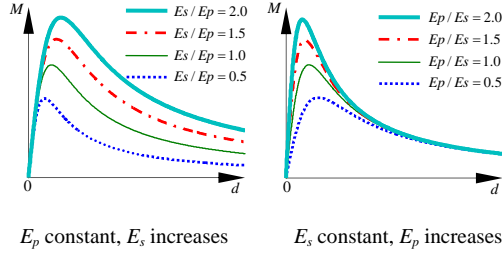
Based on Eq.(8), the relationship between the moment M and the distance d , which corresponds to the depth of the embedded piezoelectric material, and the relationship between the moment M and the half thickness of the piezoelectric material t can be presented as Fig. 3. It is shown in the Fig. 3 that the moment M increases at first with the increase of both d and t , and after reaching a maximum value, decreases with increasing d or t . This behaviour indicates that an optimal thickness and depth exist, at which point the moment M reaches a maximum value. Fig. 3 also implies the influence of the elastic moduli of the base material and of the piezoelectric material to the moment M as well as to the optimal values of d and t .

Considering only the distance d , which corresponds to the depth of the embedded piezoelectric material, the maximum moment can be reached when

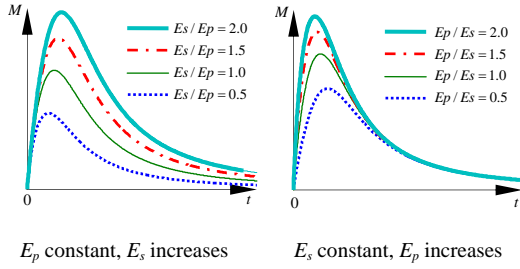
$$d = d^* = \sqrt{\frac{E_s B T^3 + E_p b t^3}{3E_p b t}} \quad (9)$$

And when the following constrain inequality is satisfied, the optimal position of the piezoelectric

materials will be inside the beam. Otherwise, the optimal position of the piezoelectric materials will be outside the beam.



(a) Relationship between M and d



(b) Relationship between M and t

Figure 3: Relationship between moment M and distance d respectively half thickness t

$$r_E \leq \frac{3r_T^2 - 6r_T + 2}{r_B r_T^3} \quad (10)$$

Where

$$r_E = E_s / E_p, \quad (11)$$

$$r_T = T / t, \quad (12)$$

$$r_B = B / b. \quad (13)$$

On the other hand, when only the half thickness of the piezoelectric materials t is taken into account, the optimal half thickness and the constrain inequality are shown as Eqs.(14) and (15), respectively.

$$t = t^* = \sqrt[3]{\frac{E_s B T^3}{2E_p b}} \quad (14)$$

$$r_E \leq \frac{2}{r_B} \quad (15)$$

Taking both of the distance d and the half thickness t into account at the same time results in the three-dimensional plots, show on the left, and contour maps, show on the right, of the moment M presented in Fig.4, with the dimensionless coordinates

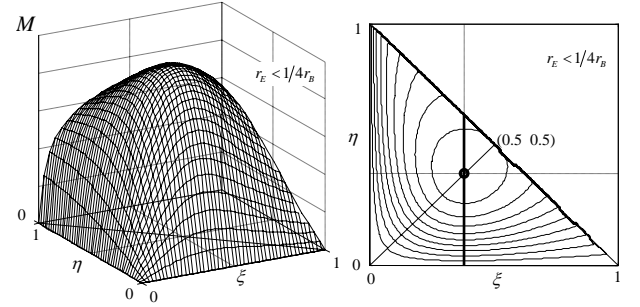
$$\left. \begin{aligned} \xi &= \frac{t}{T}, \\ \eta &= \frac{d}{T}. \end{aligned} \right\} \quad (16)$$

Under this situation, the optimal distance d^* equals to the optimal thickness t^* , which is shown as

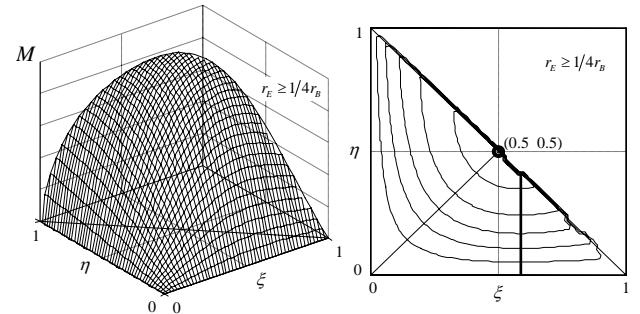
$$d^* = t^* = \sqrt[3]{\frac{E_s B T^3}{2E_p b}}. \quad (17)$$

And the constrain inequality (18) makes sure that the piezoelectric materials is embedded inside the beam, when both the distance d and thickness t get the optimal value shown in Eq.(17).

$$r_E \leq \frac{1}{4r_B} \quad (18)$$



(a) Constraint is satisfied



(b) Constraint is not satisfied

Figure 4: Three-dimensional plots and contour maps of the moment M

5 Conclusions

Figures 3 and 4, as well as constrain inequalities (10), (15) and (18), tell us that the optimal result depends on r_E , the ratios of the elastic moduli of the base material and of the piezoelectric material. With the increasing of r_E , the optimal depth and thickness also increase. When both the depth and thickness achieve their optimal values and with the satisfaction of inequality (18), the position of the piezoelectric actuator

makes one surface of the piezoelectric material just lie on the neutral plane of the beam structure. This feature is shown in the contour maps with the optimal solutions are on the line of $\xi = \eta$. The optimal results can be obtained use Eq.(17).

It is a critical quantity when $r_E = 1/4r_B$. The optimal thickness reaches the maximal value, half thickness of the beam structure, at this critical point. And the corresponding optimal depth is a quarter of thickness of the beam structure. With r_E still increasing, the optimal solution keeps the same, which is shown in the contour map with the point (0.5, 0.5) when constrain not satisfied, that is $r_E \geq 1/4r_B$.

When the inequality (18) is satisfied but the optimal thickness of piezoelectric material can not be satisfied due to other reasons, the optimal depth under this situation can also be obtained with only the depth in consideration, shown as Eq.(9), in which the thickness of the piezoelectric material plays also a role. It means that the optimal depths are different for the different thicknesses. On the other hand, Eq.(14) shows the solution with only the thickness is considered when the depth is however already fixed due to other factors. What should be pointed out is that the optimal thickness for certain r_E is always the same value, no matter how deep the piezoelectric material is embedded. This can be proofed by both the contour maps, on which the optimal solutions form a vertical line in the constrained field, and Eq.(14), in which the depth is not included. This useful information can be obtained from the three-dimensional plots and contour maps too.

The above conclusions show us that the position, corresponding with the thickness and depth, of the embedded piezoelectric material, as well as the modulus ratios between the base material and piezoelectric material are very important for the smart beam structures when the piezoelectric element is used for actuation purpose. This paper aims to give some useful instructions for constructing smart composite material beams with piezoelectric elements embedded inside the structures to serve as actuators.

6 Extension to the case of smart plates

The above results are derived from beam structures with embedded piezoelectric material, and can not be used to the case of smart plates directly. The stress of the plate is shown as

$$\left. \begin{aligned} \sigma_x &= \frac{E_s y}{(1-\nu_s^2)} \left(\frac{1}{\rho_x} + \nu_s \frac{1}{\rho_z} \right), \\ \sigma_z &= \frac{E_s y}{(1-\nu_s^2)} \left(\frac{1}{\rho_z} + \nu_s \frac{1}{\rho_x} \right). \end{aligned} \right\} \quad (19)$$

Here, the thickness direction of the plate is defined as y axes. ν_s is the Poisson ratio of the base material, and ρ_x

and ρ_z are the curvature radii of the plate structure in x and z direction, respectively. With the suppose that the deformation in both x and z direction are symmetrical, which means

$$\rho_x = \rho_z. \quad (20)$$

And when they are written as ρ , the stress is then expressed as

$$\sigma_x = \sigma_z = \frac{E_s y}{\rho(1-\nu_s)}. \quad (21)$$

The stress in the piezoelectric material is accordingly

$$\sigma_p = \frac{E_p y}{\rho(1-\nu_p)} - \frac{E_p d_{31} \mathbf{E}}{1-\nu_p}. \quad (22)$$

Here the subscript p refers to the corresponding parameters of the piezoelectric material. Comparing Eqs. (2) and (3) with Eqs. (21) and (22), it is obvious that by replacing the elastic moduli E_s and E_p by $E_s / (1-\nu_s)$ and $E_p / (1-\nu_p)$, respectively, all of the results can be applied to the case of plate structures with embedded piezoelectric actuators. The parameter (11) is now for the case of smart plate redefined as

$$r_E = \frac{E_s (1-\nu_p)}{E_p (1-\nu_s)}. \quad (23)$$

Acknowledgments

This paper is done with the cooperation of Prof. Jiesheng Jiang, Institute of Vibration Engineering, Northwestern Polytechnical University, Xi'an, China. The authors would like to express their sincere appreciation for his theoretical support.

References

- [1] Janocha, H. (Ed.), *Adaptronics and Smart Structures*, Springer publishing house Berlin Heidelberg, 1999.
- [2] Schwinn, A. and Janocha, H., Robust Control Design for an Active Vibration Suppression System. *Mechatronics 2002, Proc. 8th Mechatronics Forum International Conference*. Enschede, Netherlands 24-26 June 2002, pp. 1028-1037.
- [3] Schwinn, A. and Janocha, H., Self-Configurable Actuator-Sensor Array for Active Vibration Suppression, *Materialweek 2000*, Munich, Germany, 25-27 September 2000.
- [4] Wu, K., Schwinn, A. and Janocha, H., Active Vibration Control Using Embedded Piezoceramics as both Actuators and Sensors, *Fifth European Conference on Noise Control*, Naples, Italy, 19-21, May, 2003.
- [5] Janocha, H. (Ed.), *Actuators - Basics and Applications*, Springer publishing house Berlin Heidelberg, 2004.